Journal of Ultrafine Grained and Nanostructured Materials
https://jufgnsm.ut.ac.ir
Vol. 55, No.1, June 2022, pp. 31-36
Print ISSN: 2423-6845 Online ISSN: 2423-6837
DOI: 10.22059/jufgnsm.2022.01.05

Can the Spacer Cation Affect the Preferential Growth and Phase Segregation in 2D Ruddlesden-Popper Perovskites?

Saeed Bayat[1], Hossein Abdizadeh*[,1,2], Mohammad Reza Golobostanfard*[,1]

[1]School of Metallurgy and Materials Engineering, College of Engineering, University of Tehran, Tehran, Iran;
[2]Center of Excellence in Materials for Low-Energy Consumption Technologies, University of Tehran, Tehran, Iran.

Recieved: 11 October 2021; Accepted: 17 January 2022

**Corresponding author email: abdizade@ut.ac.ir , bostanfr@ut.ac.ir*

ABSTRACT

Organic-inorganic halide perovskites (OIHP) are an emerging family of semiconductor materials widely used in the fabrication of optoelectric devices, including solar cells, due to their superior optical and electrical properties. Poor long-term stability of OIHPs is the main hindrance to the commercialization of perovskite solar cells. Using 2D Ruddelsden-Popper perovskites is a common approach to improve perovskite solar cell stability. However, their 2D structure restricts the transport of charges, thus reduces the photovoltaic performance of perovskite solar cells. Out-of-plane growth of 2D perovskite film can significantly improve carrier transport and consequently reduces the rate of non-radiative recombination. One of the main factors that affects the preferential growth of 2D perovskites is the type of spacer cation that exists in the 2D perovskites structure. Herein, butylammonium (BA^+) and phenetylammonium (PEA^+) spacer cations, as well as their combination, are employed in 2D perovskite thin film, and their effects on preferential growth and phase segregation have been investigated. X-ray diffraction (XRD) data shows that the BA-based 2D perovskite has a more desirable (220) preferential direction, but the preferred peaks of PEA-based 2D perovskite have higher intensity and narrower full width at half maximum (FWHM) than the BA-based counterparts, which is due to the rigid nature of the PEA^+ compared to the BA^+ molecule. It is also observed that the replacement of BA^+ instead of PEA^+ significantly reduces phase segregation. This phenomenon is probably related to the phenyl ring of the PEA^+ molecule, which is entirely solvophobic and slows down the formation of DMF.PEAI complex during the crystallization step, which in turn leads to the formation of small n 2D perovskite nucleus causing phase segregation. SEM images also represent that the BA, PEA-based film has a smoother surface and lower pinholes than the PEA and BA-based 2D perovskite.

Keywords: *2D perovskite, Ruddelsden-Popper, Butylammonium, Phenetylammonium, Preferential growth.*

1. Introduction

Organic-inorganic halide perovskites (OIHPs) are an emerging family of semiconductor materials that have attracted the attention of scientists due to their glamorous and promising optoelectric properties such as high carrier mobility, high absorption coefficient, low Urbach energy (3-4 meV) [1], acceptable exciton binding energy (15.9-425 meV) [2], suitable and tuneable bandgap (1.1-2.5 eV) [3], low trap state density (< 1.12×10^{15}) [4], and cheap and low-temperature processing [5]. Due to the mentioned properties, the power conversion efficiency (PCE) of perovskite solar cells has increased with a very steep slope from 10.9% in 2012 to 25.6% in 2021 [6], [7]. However, even the most efficient perovskite solar cells suffer from instability, originating from thermal decomposition, photoinduced degradation, and

moisture instability [8]. Many efforts have been made to improve the stability of perovskite solar cells, and hence different strategies have been used for this purpose, including compositional engineering, interface engineering, and encapsulation. One of the promising approaches to increase the intrinsic withstanding of perovskite solar cells under ambient conditions is using the low dimensional perovskite structures as the active layer.

2D perovskites are a new category of perovskite materials that have been developed in recent years. The most common 2D perovskites which are used in optoelectric devices are the <100> oriented 2D perovskites. The general formula of <100> oriented 2D perovskites is $A'_mA_{n-1}B_nX_{3n+1}$ (in which A' is a large spacer cation, A is a monovalent organic or inorganic cation such as methylammonium (MA^+) or formamidinium (FA^+) or cesium (Cs^+), B is a divalent inorganic cation usually Pb^{2+}, and X is halogen anion such as I^-, Br^-, or Cl^-). In this formula, n is the thickness of inorganic layers separated by spacer cations, and m is the number of spacer molecules that separate the inorganic layers in the single unit cell of 2D perovskites. <100> oriented 2D perovskites are divided into three main groups based on the valence of spacer cations, including Ruddelsden-Popper (RP) (m=2), Dion-Jacobson (DJ) (m=1), and alternating cations in the interlayer spacer (ACI), that among them, 2D RP perovskite has excellent stability against the three main sources of degradation, because of its outstanding moisture stability and high negative Gibbs free energy of formation [9].

Despite the high stability of 2D RP perovskite-based solar cells, they still suffer from low PCE. This weakness of PCE is related to the wide bandgap and intrinsic poor charge transport of the 2D RP perovskite absorber layer. The charge transport of 2D RP perovskite is highly dependent on the orientation of the perovskite film. The out-of-plane orientation of 2D perovskite thin film can accelerate the charge transport [9]. There are a lot of approaches to improve the out-of-plane orientation of 2D perovskite, including preheating process [10], additives [11-13] and solvent engineering [11], vacuum poling [12], compositional engineering [13]. The molecular structure of spacer cations is one of the most important parameters of the orientation of 2D perovskite thin film [14].

Butylammonium (BA^+) $(CH_3(CH_2)_3NH_3)^+$ and phenetylammonium (PEA^+) $(C_6H_5NH_3)^+$ are the most common spacer cations that are widely used in 2D RP perovskite-based photovoltaic devices due to their affordable cost and acceptable optoelectric properties [14]. 2D RP perovskite thin films based on BA^+ have more desirable preferential orientation in (220) orientation (in the low amount of (n)) due to their small size (compared to (PEA^+)), flexible molecular structure, and different growth kinetic [15]. Nevertheless, (BA^+) based 2D perovskites have a wider bandgap compared with PEA^+ counterparts. On the other hand, PEA-based 2D perovskites have a lower bandgap compared to BA^+ based counterparts due to the robust nature of the phenyl ring of PEA^+ molecule and larger size than BA^+, which leads to absorption of a broader range of the solar spectrum suitable for photovoltaic applications [15].

In this work, we provide insight into the mode of secondary spacer cation intervention on preferential growth and phase segregation of 2D RP perovskite film. The synergistic effect of PEA^+ and BA^+ on the preferential growth and preferential orientation of 2D RP thin film is studied. On the other hand, the mechanism of phase segregation during the crystallization process is discussed.

2. Experimental details

2.1. Materials

Anhydrous dimethyl sulfoxide (DMSO, 99.9%), N,N-dimethylformamide (DMF, 99.8%), lead iodide (PbI_2, >99%), and phenethylammonium iodide (PEAI, 99.9) were all purchased from Sigma-Aldrich, and anhydrous methylammonium iodide (MAI, 99.99%) and butylammonium iodide (BAI 99.9) were purchased from Dyesol. Anhydrous titanium (IV) isopropoxide (TTIP, 97%), hydrochloric acid (HCl), and 1-propanol (1PrOH) were purchased from Merck. All chemical compounds were used without any further purification process.

2.2. Film fabrication

The perovskite film was deposited on the 1.4*1.4 cm glass substrate. The substrates were cleaned with deionized water (DIW) and ethanol, then immersed in ethanol for 30 min into the ultrasonic bath, and after drying, treated in UV-ozone for 30 min. The anatase hole blocking layer was applied on cleaned glass based on the previous report [16].

To prepare n=3 2D RP perovskite precursor solutions, a suitable amount of PbI_2 was dissolved in DMF:DMSO (4:1 volume ratio) and stirred for 10 min under 100 °C. Then the MAI, PEAI, and

BAI were added to the precursor solution and stirred for 10 min (the molar ratio of (PEA_xBA_{1-x}): $MAI:PbI_2$ was 2:2:3, and the concentration of all solutions were 70 wt% and same for example, in the PEA-based sample 500 µl of precursor solution by PEAI (0.7179 g), MAI (0.1650 g), and PEAI (0.2586 g) was prepared). Finally, 50 µl of perovskite precursor solution was deposited on the preheated substrate (100 °C) by the spin coating method (4000 rpm for 30 sec) without any antisolvent process, and the pristine film was annealed at 100 °C for 10 min under ambient atmosphere.

2.3. Characterization

X-ray diffraction method (XRD, Philips X-pert pro, PW1730) with Cu Kα radiation (λ = 1.5418 Å, 40 kV, 30 mA) in the range of 10° < 2θ < 40° was carried out to study the crystal structure of the 2D RP perovskite films, and morphological aspects were analyzed by field-emitted scanning electron microscopy (FESEM, MIRA3 TESCAN).

3. Results and discussion

As mentioned, the growth direction of inorganic sheets in 2D RP perovskite has a considerable impact on charge transport and PCE of 2D perovskite-based solar cells. Fig.1-a shows the crystal structure of n=3 2D RP perovskite. As it can be seen in Fig.1-a, the (0k0) orientation of inorganic sheets, which is called in-plane orientation, disrupts carrier transport toward charge transport layers. Instead, (111) and especially (220) orientation (or out-of-plane orientation) leads to facilitation of charge transport [17]. One of the most critical factors affecting the preferential growth of 2D RP perovskites is the type of spacer cation [14]. Using a suitable secondary spacer cation is an effective and simple method for improving the preferential growth of 2D RP perovskite. To determine the effect of Secondary Spacer Cations (SSC^+) on the crystallographic structure of 2D RP perovskite film, the XRD pattern of $(PEA)_2(MA)_2Pb_3I_{10}$, $(BA)_2(MA)_2Pb_3I_{10}$, and $(PEA)(BA)(MA)_2Pb_3I_{10}$ are shown in Fig.1-b. As can be seen, the peak position of 14.2° and 28.5° that are related to the (111) and (220) planes, are the prominent peaks in all samples [18]. It shows that the out-of-plane growth is dominant in all samples. However, the low-intensity peaks belong to (0k0) planes can be seen in the $(PEA)_2(MA)_2Pb_3I_{10}$ pattern, which is represented the in-plane growth of 2D RP perovskite. It is also illustrated that there is a slight peak shift for $(PEA)(BA)(MA)_2Pb_3I_{10}$ compared to both other samples. This peak shift is related to the

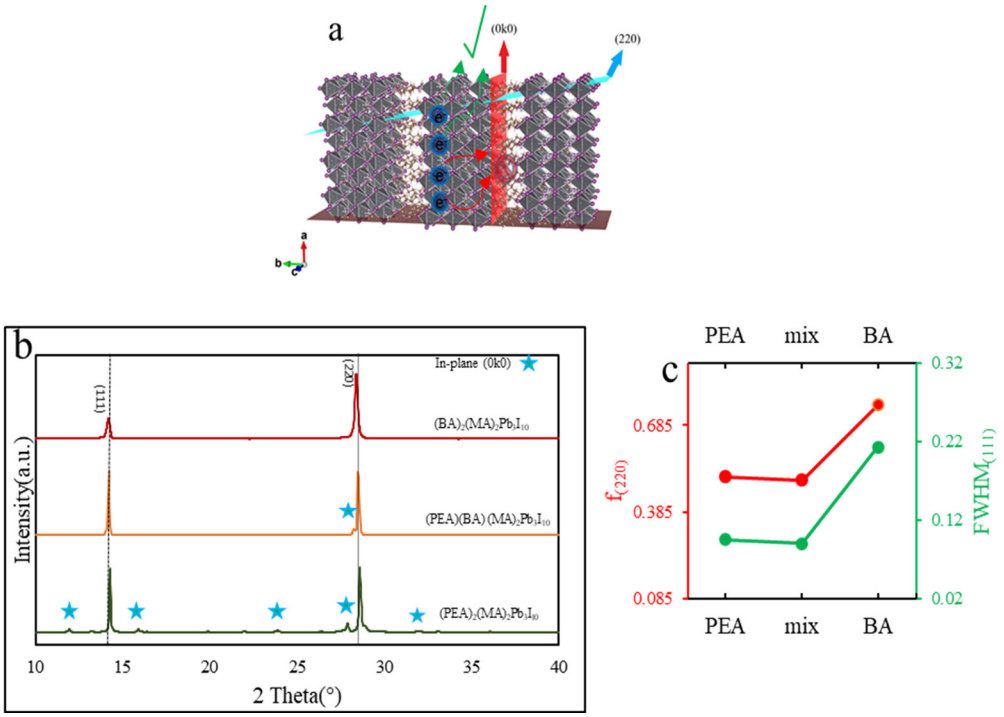

Fig. 1- a) The schematic figure of out-of-plane orientation and charge transport routes, b) The XRD patterns of the samples, and c) The full width at half maximum of (111) plane ($FWHM_{(111)}$) and the relative (220) orientation ($f_{(220)}$) of samples.

size difference between BA^+ and PEA^+. Because of the robust phenyl ring in PEA^+ molecules, the size of PEA^+ molecules is larger than BA^+; therefore, the lattice constant and d-spacing of $(PEA)_2(MA)_2Pb_3I_{10}$ phase ($d_{(111)}$=6.248 Å) is larger than the BA-based phase ($d_{(111)}$=6.214 Å), and according to Bragg equation ($n\lambda=2d\sin\theta$), the peak position of (111) is shifted to lower angle (about -0.12°). In (PEA)(BA)$(MA)_2Pb_3I_{10}$ sample, the peak position of (111) plane is shifted about -0.04° compared to PEA-based and +0.08 compared to BA-based sample ($d_{(111)}$=6.240 Å). It represents the simultaneous presence of PEA^+ and BA^+ in the structure of (PEA)(BA)$(MA)_2Pb_3I_{10}$ sample.

In order to determine the amount of crystallinity of the samples, Fig1-c shows the full width at half maximum of (111) plane ($FWHM_{(111)}$), which is extracted by Gaussian function fitting. It is clear that the $FWHM_{(111)}$ of the BA-based sample is higher than the PEA counterpart. This is probably due to the poor crystallinity of the BA-based sample compared to other samples. However, it can be seen that the $FWHM_{(111)}$ of (PEA)(BA)$(MA)_2Pb_3I_{10}$ sample is lower than other samples. On the other hand, the relative (220) orientation ($f_{(220)}$) of samples obtained according to eq.1:

$$f_{(220)} = \frac{I_{(220)}}{I_{(220)}+I_{(111)}} \quad (1)$$

As mentioned, the (220) orientation of the inorganic sheet represents the better out-of-plane orientation of perovskite film [19]. It can be seen in Fig.1-c that the $f_{(220)}$ of the BA-based sample is higher than other samples that might be related to the different kinetics of growth of BA-based film that was reported previously [17]. However, it is illustrated that the $f_{(220)}$ of (PEA)(BA)$(MA)_2Pb_3I_{10}$ is lower than the other samples (even PEA-based sample). As mentioned above, the (220) orientation is the more desirable orientation for high efficient charge transport, which is dominant in the BA-based sample. In (PEA)(BA)$(MA)_2Pb_3I_{10}$ sample, the low (220) orientation shows that the dominant orientation is not (220), but because of low FWHM compared to the BA-based sample, the total amount of preferred planes in this sample is higher than BA-based sample [17].

Fig.2 illustrates the FESEM images of 2D RP perovskite samples. It can be seen that the FESEM image of the BA-based sample displays the rough surface, which is related to the rapid crystallization kinetics of BA-based 2D perovskite. On the other hand, the PEA-based sample possesses dense and packed grains with a very coarse average grain size (about 4 μm while it measured 3.5 μm and 2 μm for PEA and BA-based samples, respectively). This very large grain size is one of the best reports about $(PEA)_2(MA)_2Pb_3I_{10}$ film that is synthesized by the spin coating method. This high average grain size represents the slow crystallization during the annealing process. But obviously, there are a few numbers of particles on the surface of the PEA-based sample (Fig.2-b), which is attributed to residual PbI_2 particles. Because of the solvophobic phenyl ring of PEA^+ molecules, PEA^+ has weak electrostatic interaction with Lewis-based solvents (especially DMF), and it is not well coordinated by solvent molecules [18]. Because of this, the complex of PEAI.DMF is not formed sufficiently during the annealing process. Then the crystallization kinetic of PEAI and PbI_2 will not be equivalent in liquid/solid interface, where the evaporation rate of solvents is high, and supersaturation of PEAI occurs rapidly. As a result, there will be a PEA+-rich region in the liquid/gas interface, which will create an extraordinary hydrophobic surface on top of the PEA-based 2D perovskite thin film that reinforces moisture stability of the 2D perovskite phase [18], [20].

Furthermore, as the evaporation process continues, the supersaturation of PbI_2 and MAI is formed under the PEA^+-rich zone. Because of the ultra-low concentration of PEA^+ molecule in this region, the 3D perovskite phase will be formed under the PEA^+-rich region according to eq.2.

$$3PbI_2 + 2MAI \Longrightarrow 2MAPbI_3 + PbI_2 \quad (2)$$

According to the stoichiometry of precursor in this sample, the molar ratio of PEAI:PbI_2:MAI is 2:3:2, indicating that in the PEA^+-poor region, for the formation of each 2 mol 3D perovskite, one mole PbI_2 will precipitate, which is also shown in eq.2. The excess PbI_2 precipitates on the surface of the film (as can be seen in Fig.2-b). The thickness of the 3D perovskite region is not too large, and because of this, the amount of precipitated PbI_2 particles is not enough to be seen in the diffraction pattern of the PEA-based sample (Fig.1-b). After the formation of the 3D perovskite region, the concentration of PEA^+ is gradually increased, and as a result, the high (n) 2D perovskite phase will be formed. Finally, as getting away from the PEA^+-poor region in the solid/liquid interface, the concentration of

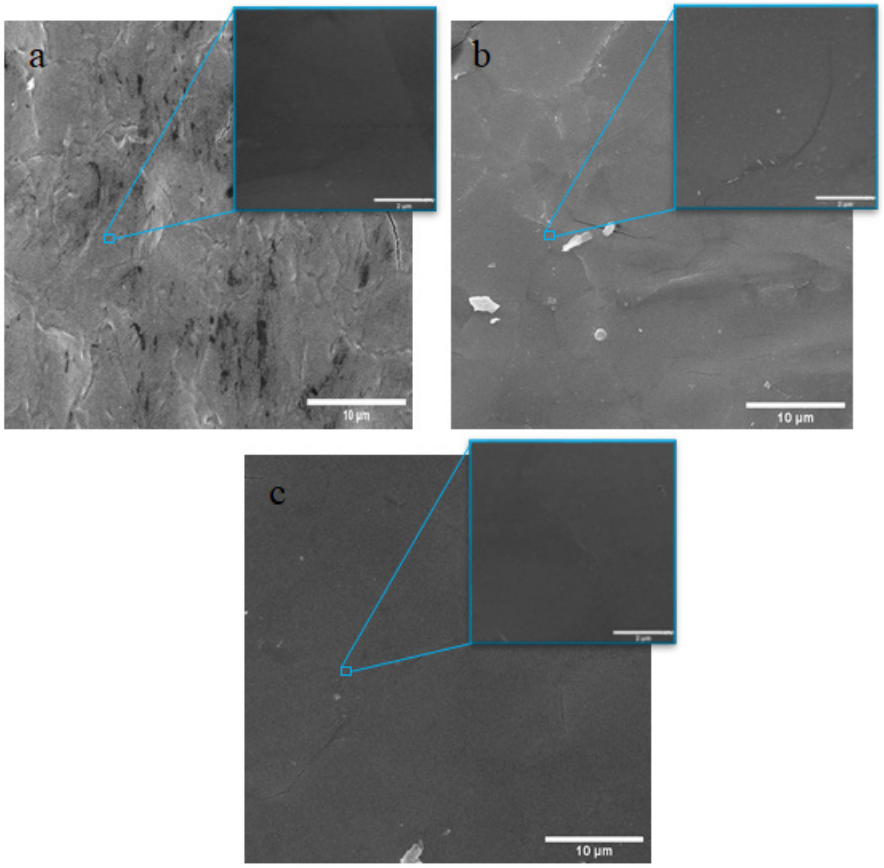

Fig. 2- FESEM image of 2D RP thin film with different spacer cation: a) $(BA)_2(MA)_2Pb_3I_{10}$, b) $(PEA)_2(MA)_2Pb_3I_{10}$, and c) $(PEA)(BA)(MA)_2Pb_3I_{10}$ (the inset is a high magnification image (×30k)).

PEA^+ rises again, and low (n) 2D perovskite will be formed. The low (n) 2D perovskite does not tend to out-of-plane growth [20]. The existence of the low (n) 2D perovskite phase with in-plane growth direction can also be seen in the XRD pattern of the PEA-based sample (Fig.1-b). Instead, the BA^+-rich zone and PbI_2 particles are not observed in the BA-based sample due to the strong interaction between the solvophilic amine group and the lack of the solvophobic agent in BA^+ molecules. But a similar gradient structure was reported about BA-based 2D RP perovskite [21].

The FESEM image of $(PEA)(BA)(MA)_2Pb_3I_{10}$ sample (Fig.2-c) indicates a very smooth, packed grain, and PbI_2 free surface that is related to the synergistic effect of the simultaneous presence of PEA^+ and BA^+ in the crystal structure of 2D perovskite which was reported previously [22]. The inappreciable amount of low (n) phase with the in-plane orientation of this sample is observed in its XRD pattern, but the perfect morphology without any segregation indicates that the presence of BA^+ is neutralized the destructive segregation effect of PEA^+ without reduction of surface quality.

4. Conclusion

In conclusion, the effect of bulky spacer cation on the phase segregation, preferential growth, and morphology of 2D RP perovskite is studied. The PEA-based sample has an excellent smooth morphology, but the BA-based sample has a non-uniform and rough surface. Instead, the phase segregation and partially in-plane orientation are observed in the PEA-based sample, which is probably related to the phenyl ring of PEA^+ molecules that acts as a solvophobic agent. On the other hand, it is observed that the (PEA)(BA)$(MA)_2Pb_3I_{10}$ sample has good uniform morphology with a segregation-free surface and a large grain size compared to other samples. The low $FWHM_{(111)}$ and the negligible amount of in-plane oriented phase in this sample indicates that the synergistic effect of two types of cation improves the crystallinity and surface quality of (PEA)(BA)

$(MA)_2Pb_3I_{10}$ thin film. Finally, it was observed that the type of spacer cation not only changes the total amount of the preferred planes but also plays a decisive role in determining the phase orientation and phase segregation of the 2DRP phase.

References

1. Ledinsky M, Schönfeldová T, Holovský J, Aydin E, Hájková Z, Landová L, et al. Temperature Dependence of the Urbach Energy in Lead Iodide Perovskites. The Journal of Physical Chemistry Letters. 2019;10(6):1368-73.
2. Passarelli JV, Mauck CM, Winslow SW, Perkinson CF, Bard JC, Sai H, et al. Tunable exciton binding energy in 2D hybrid layered perovskites through donor–acceptor interactions within the organic layer. Nature Chemistry. 2020;12(8):672-82.
3. Jena AK, Kulkarni A, Miyasaka T. Halide Perovskite Photovoltaics: Background, Status, and Future Prospects. Chemical Reviews. 2019;119(5):3036-103.
4. Ding M, Sun L, Chen X, Luo T, Ye T, Zhao C, et al. Air-processed, large grain perovskite films with low trap density from perovskite crystal engineering for high-performance perovskite solar cells with improved ambient stability. Journal of Materials Science. 2019;54(18):12000-11.
5. Roy P, Kumar Sinha N, Tiwari S, Khare A. A review on perovskite solar cells: Evolution of architecture, fabrication techniques, commercialization issues and status. Solar Energy. 2020;198:665-88.
6. Lee MM, Teuscher J, Miyasaka T, Murakami TN, Snaith HJ. Efficient Hybrid Solar Cells Based on Meso-Superstructured Organometal Halide Perovskites. Science. 2012;338(6107):643-7.
7. Jeong J, Kim M, Seo J, Lu H, Ahlawat P, Mishra A, et al. Pseudo-halide anion engineering for α-FAPbI3 perovskite solar cells. Nature. 2021;592(7854):381-5.
8. Boyd CC, Cheacharoen R, Leijtens T, McGehee MD. Understanding Degradation Mechanisms and Improving Stability of Perovskite Photovoltaics. Chemical Reviews. 2019;119(5):3418-51.
9. Zhang F, Lu H, Tong J, Berry JJ, Beard MC, Zhu K. Advances in two-dimensional organic–inorganic hybrid perovskites. Energy & Environmental Science. 2020;13(4):1154-86.
10. Tsai H, Nie W, Blancon J-C, Stoumpos CC, Asadpour R, Harutyunyan B, et al. High-efficiency two-dimensional Ruddlesden–Popper perovskite solar cells. Nature. 2016;536(7616):312-6.
11. Zhang J, Zhang L, Li X, Zhu X, Yu J, Fan K. Binary Solvent Engineering for High-Performance Two-Dimensional Perovskite Solar Cells. ACS Sustainable Chemistry & Engineering. 2019;7(3):3487-95.
12. Zhang J, Qin J, Wang M, Bai Y, Zou H, Keum JK, et al. Uniform Permutation of Quasi-2D Perovskites by Vacuum Poling for Efficient, High-Fill-Factor Solar Cells. Joule. 2019;3(12):3061-71.
13. Zhou N, Shen Y, Li L, Tan S, Liu N, Zheng G, et al. Exploration of Crystallization Kinetics in Quasi Two-Dimensional Perovskite and High Performance Solar Cells. Journal of the American Chemical Society. 2018;140(1):459-65.
14. Parikh N, Tavakoli MM, Pandey M, Kalam A, Prochowicz D, Yadav P. Role of the spacer cation in the growth and crystal orientation of two-dimensional perovskites. Sustainable Energy & Fuels. 2021;5(5):1255-79.
15. Quintero-Bermudez R, Gold-Parker A, Proppe AH, Munir R, Yang Z, Kelley SO, et al. Compositional and orientational control in metal halide perovskites of reduced dimensionality. Nature Materials. 2018;17(10):900-7.
16. Golobostanfard MR, Abdizadeh H. Influence of carbon nanotube wall thickness on performance of dye sensitized solar cell with hierarchical porous photoanode. Microporous and Mesoporous Materials. 2014;191:74-81.
17. N. Zhou, B. Huang, M. Sun, Y. Zhang, L. Li, Y. Lun, X. Wang, J. Hong, Q. Chen, and H. Zhou, "The Spacer Cations Interplay for Efficient and Stable Layered 2D Perovskite Solar Cells," Adv. Energy Mater., vol. 10, no. 1, pp. 1–13, 2020, doi: 10.1002/aenm.201901566.
18. Lian X, Chen J, Zhang Y, Qin M, Andersen TR, Ling J, et al. Solvation effect in precursor solution enables over 16% efficiency in thick 2D perovskite solar cells. Journal of Materials Chemistry A. 2019;7(33):19423-9.
19. Hu S, Yang X, Yang B, Zhang Y, Li H, Sheng C. Excitonic Solar Cells Using 2D Perovskite of (BA) 2 (FA) 2Pb3I10. The Journal of Physical Chemistry C. 2021 Jan 19;125(3):2212-9.
20. Xu Y, Wang M, Lei Y, Ci Z, Jin Z. Crystallization Kinetics in 2D Perovskite Solar Cells. Advanced Energy Materials. 2020;10(43):2002558.
21. Kheirabadi H, Abdizadeh H, Golobostanfard MR. Boosting the Graded Structure of 2D Perovskite Solar Cell Based on $BA_2MA_{n-1}Pb\ nI_{3n+1}$ by Noninteger n Values. ACS Applied Energy Materials. 2020;4(1):394-403.
22. Lian X, Chen J, Qin M, Zhang Y, Tian S, Lu X, et al. The Second Spacer Cation Assisted Growth of a 2D Perovskite Film with Oriented Large Grain for Highly Efficient and Stable Solar Cells. Angewandte Chemie International Edition. 2019;58(28):9409-13.